Experiments in Fluids 20 (1996) 441–453 © Springer-Verlag 1996

The velocity field of the turbulent very near wake of a circular cylinder

L. Ong, J. Wallace

Abstract Hot-wire measurements were conducted in the very near wake ($x/d \leqslant 10$) of a circular cylinder at a Reynolds number based on cylinder diameter, Re_d of 3900. Measurements of the streamwise velocity component with the use of single sensor hot-wire probes were found to be inaccurate for such flowfields where high flow angles are present. An X-array probe provided detailed streamwise and lateral velocity component statistics. Frequency spectra of these two velocity components are also presented. Measurements with a 4-sensor hot-wire probe confirmed that the very near wake region is dominantly two-dimensional, thus validating the accuracy of the present X-array data.

1 Introduction

The flow past a circular cylinder is one of the most extensively studied flowfields. The sub-critical Reynolds number range of 300 to 2×10^5 is of particular interest to investigators of coherent eddies and turbulent transport, because it is in this range that transition to turbulence occurs naturally in the separated free shear layers. However, experimental data in the very near wake region, x/d less than 10, for this sub-critical Reynolds number range is very rare in the literature. This is undoubtedly due to the high velocity vector angles of attack coupled with relatively low streamwise velocity magnitudes which makes velocity measurements in this region of the wake, especially with hot-wire probes, extremely difficult (see Sect. 7). Most experimental studies are either near the cylinder surface (e.g. Roshko 1954; Achenbach 1968; Farell and Blessmann 1983) or at x/d greater than 10 (e.g. Townsend 1947, 1949a, b; Yamada et al. 1980; Wygnanski et al. 1986; Zhou and Antonia 1993). Bouard and Coutanceau (1980), using a flow visualization technique, studied the development of the velocity profiles for an impulsively started cylinder for the Reynolds number range of 40–10^4. Bloor and Gerrard (1966) studied the evolution of vortices in a circular cylinder wake for the Reynolds number range of 10^3 to 4×10^4. Using a single-sensor hot-wire probe, they obtained mean streamwise velocity and turbulent intensities profiles, and also obtained an estimation of the vortex speed. The experiment of Cantwell and Coles (1983), who used a flying hot-wire technique, provided detailed phase averaged velocity and Reynolds stress data in the very near wake, but at a high sub-critical Reynolds number of 1.4×10^5.

The primary motivation for this study was the need for experimental data with which to validate Large-eddy simulations (LES) of the near wake of a circular cylinder that were carried out by Beaudan and Moin (1994) at the Center for Turbulence Research, NASA Ames Research Center. Their study concluded that the LES that used the dynamic subgrid-scale eddy-viscosity model yielded better accuracy in the vortex formation region of the cylinder wake compared to the simulations which used no subgrid scale model or the fixed coefficient Smagorinsky model. They also concluded that even high-order (up to 7^{th} order) accurate upwind numerical schemes are not suitable for such complex flowfields, because they are overly dissipative.

Hence, the purposes of this paper are two-fold: (1) to explore the limitations of hot-wire probe measurement methods in turbulent flows with large instantaneous angles of attack of the velocity vector to the probe sensors and (2) to carry out, with the method determined to be the best, a detailed investigation in the very near wake ($x/d \leqslant 10$) of a circular cylinder. The velocity field statistical properties at Reynolds number, Re_d, of 3900, where d is the cylinder diameter and x is the direction of the free stream flow, were measured and compared to the results of the LES of Beaudan and Moin (1994) at the same Reynolds number and x/d locations and, at x/d of 10, to the X-array wire measurements of Zhou and Antonia (1993).

Preliminary measurements with a single sensor probe, in the very near wake of a circular cylinder, yielded unphysically high streamwise velocity fluctuations, u. This led us to carry out a detailed analysis of the accuracy of single and X-array hot-wire probes measurements for flows with high angles of attack. Following this analysis, the use of a single-sensor probe for the present study was abandoned in favor of X-array probes. A brief comparison between two methods for reducing X-array data, i.e. the Cosine-law and the Look-Up Table (LUT) techniques, was also performed.

Received: 28 April 1995/Accepted: 13 November 1995

L. Ong, J. Wallace
Department of Mechanical Engineering, University of Maryland, College Park, MD 20742, USA

Correspondence to: L. Ong

This study has been funded by the NASA-Ames University Consortium Cooperative Agreement, NCC2-5003. We wish to thank Patrick Beaudan for providing us with the LES results for comparison and Parviz Moin for his interest in and encouragement of this experiment to provide validation data for the LES. We also wish to thank Joseph Murray for his help with the look-up-table data reduction program.

A set of wake velocity profiles have been obtained at several stations downstream of the circular cylinder: $x/d = 3, 4, 5, 6, 7$ & 10. Statistical properties of the streamwise, u, and lateral, v, fluctuating velocity components, the u and v frequency spectra, and an estimate of the spanwise correlation length are presented. Additionally, simultaneous measurements of all three velocity components were made with a 4-sensor probe along the wake centerline. The 4-sensor probe used here has an approximate sensing area of 1 mm × 1 mm, which is about twice as large as the X-array probe used for the detailed measurements. This set of measurements was conducted to explore the extent of the three-dimensionality of the wake and thus to provide a semi-quantitative validation of the X-array measurements which, of necessity, assume a two-dimensional flowfield.

2
Experimental apparatus and procedure

The experiments were conducted in the wind tunnel of the Turbulence Research Laboratory, University of Maryland. The test-section of the windtunnel has a rectangular cross-section of 1.2 m width and 0.7 m height. A circular cylinder, with a diameter of 14.3 m, was mounted at approximately 7.3 m from the end of the contraction and at the tunnel's half-height location The cylinder's axis was aligned in the spanwise direction. A three-directional traversing device enabled motor-driven probe positioning in the y and z directions and manual probe positioning in the x-direction. The same coordinate system, listed in Table 1, is used for both the flow facility and the probe (see also Fig. 1). Herein, uppercase variables denote instantaneous values, lowercase variables denote fluctuations about average values, overbars denote time averaged values, and superscript primes denote rms values.

Table 1. Coordinate axis and associated velocity components.

Coordinate axis	Velocity component	Nomenclature used
x	U	Streamwise (mean flow direction)
y	V	Lateral (normal to the cylinder's axis)
z	W	Spanwise (parallel to the cylinder's axis)

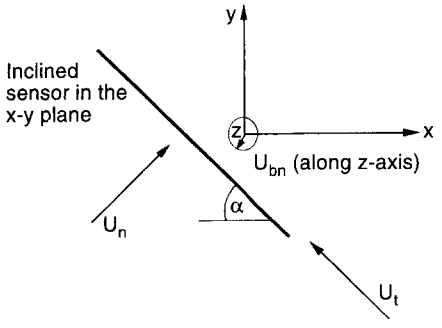

Fig. 1. Probe coordinate system

The hot-wire probes were operated in the constant temperature mode with A.A. Lab Systems Hot-wire Anemometer circuits at overheat ratios of 1.2 and 1.35, for the 4-sensor and X-array probes respectively. The tunnel velocity was monitored using a pitot-static probe connected to a Barocel Electronic Manometer with a range of 0–1 Torr and a resolution of 10^{-5} Torr. The uncertainty in absolute velocity value is approximately ± 0.05 m/s (or about $\pm 1\%$ of the freestream velocity).

The outputs of the anemometer channels were digitized by an Optim Megadac 5018 16-bit Data Acquisition System which has a maximum data throughput of 250 kHz. This system was controlled by a personal computer via an IEEE 488 interface. The digitized data were immediately streamed to the PC's hard disk for temporary storage. The acquired data sets were subsequently transmitted to a Sun Microsystem's workstation for further data analysis and archival storage on tape.

A compact, compressed-air driven jet was used to calibrate the hot-wire probes. This jet, with a circular exit nozzle diameter of 30 mm and a contraction ratio of 2.56, is mounted on a motorized angular displacement mechanism, enabling automated probe calibration for pitch and/or yaw responses. The jet's pitch and yaw axis is centered along it's longitudinal axis and located approximately 5 mm from the jet exit plane. Probes to be calibrated are placed approximately at this center of rotation, which is well within the jet's irrotational and uniform flow core region. The pressure drop across the nozzle was pre-calibrated against the flow speed (measured with a pitot-static tube), and was used to monitor the jet's exit flow speed. The freestream velocity of the wake was, $U_\infty \approx 4.2$ m/s which gave a Reynolds number based on cylinder diameter of $Re_d \approx 3900$. The freestream turbulence intensity was 0.67%. The data were digitized at 6912 Hz, with a pre-digitization analog low-pass filter cutoff frequency of 2564 Hz.

The X-array hot-wire sensors, used for this experiment, are approximately 0.6 mm long. The sensors are spaced 0.4 mm from each other in the binormal direction and are oriented at angles of approximately $\pm 40^\circ$ from the x-axis. For reasons to be described in the following sub-section, the Look-Up-Table technique of Gresko (1988) was used to reduce the definitive X-array data presented herein. A brief analysis of the effects due to bi-normal cooling on X-array data is also given below.

3
Experimental evaluation of errors due to bi-normal cooling

It is well known that a single sensor hot-wire, operated alone, cannot distinguish between the changes in the velocity magnitude and changes in the flow direction. For an ideal single-sensor hot-wire, the effective cooling velocity is simply the flow velocity vector resolved in the direction normal to the sensor and parallel to the support prongs. For a single sensor oriented to the flow at a pitch angle, ϕ, Bradshaw (1971) defined this concept as the 'Cosine Law' for effective cooling:

$$U_{\text{eff}} = U \cos \phi. \tag{1}$$

When the flow towards the sensor is at an arbitrary angle, then the velocity vector can be resolved into the normal, binormal, and tangential velocity components, as shown in Fig. 1. In practice, the presence of the hot-wire support prongs, the

length of the sensor, and other physical effects must be taken into account. Researchers (e.g. Champagne et al. 1967a, b; Jorgensen 1971; Müller 1982) have attempted to correct for these physical effects by introducing certain correction factors that only can be obtained through calibration. One must bear in mind that these correction factors (or calibration coefficients) are unique for each probe. In order to measure the turbulence intensities and/or the Reynolds stresses, these methods often involve multi-orientations of the probes and the neglection of higher order terms or correlations. These methods are restricted to use in flows with low turbulence intensities ($<10\%$) and low flow angles.

3.1
Single-sensor (normal) hot-wire probe results

In this evaluation, the calibrated (at zero pitch and yaw angles) single-sensor probe was placed in the potential core flow of the calibration jet, which was re-oriented at a variety of pitch and yaw angles relative to the probe's axis. The sensor axis was oriented in the y-direction of Fig. 1 so that yawing the jet caused binormal cooling. Figure 2 shows the error incurred at various pitch and yaw angles when it is assumed that $U \approx U_{\text{eff}}$, i.e. that no tangential and binormal cooling occurs because they cannot be accounted for by a single sensor. This plot shows that for yaw angles of $< \pm 5°$, the estimate of the streamwise velocity component U is within 5% for the whole range of pitch angles of $\pm 25°$. At higher yaw angles, the error incurred with this assumption is much greater, viz. 20–25% at yaw angle of about $\pm 30°$. Three-dimensionality, i.e. non-zero pitch for a given yaw, increases the inaccuracy. As expected, U is always overestimated at all non-zero yaw angles because U_{eff} physically accounts for the induced flow magnitude as discussed below.

The plot in Fig. 3 represents the difference between the magnitude of the induced velocity and U_{eff} obtained using the calibrated single sensor probe when it is not aligned with the induced flow direction. Such lack of alignment is unavoidable when a probe is placed in an unknown two or three dimensional mean flowfield. Increasing the yaw angle resulted in an increase of the percentage error due to binormal cooling effects. Compared to the much larger error in recovering the U-velocity component, where errors can be greater than 25% at the extreme yaw angles, the error curves in this plot are limited on a $\pm 10\%$ band throughout the pitch and yaw angle ranges examined here. This result indicates that a single sensor probe performs quite adequately (within $\pm 10\%$ for pitch and yaw angles less than $\pm 25°$) as a velocity magnitude measurement device. This plot also shows the expected decrease in cooling efficiency with increasing pitch angle, e.g. at a yaw angle of 0° the error is negative for pitch angles greater than 0°.

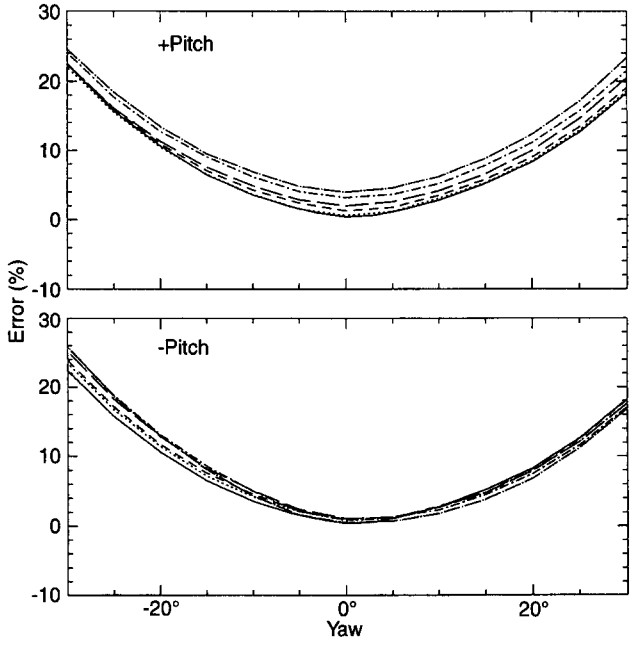

Fig. 2. Error in single hot-wire measurements of the streamwise velocity component as a function of yaw angle at selected pitch angles [°]: —— 0, ·····5, - - - 10, – – – 15, – · – , 20, — · —25

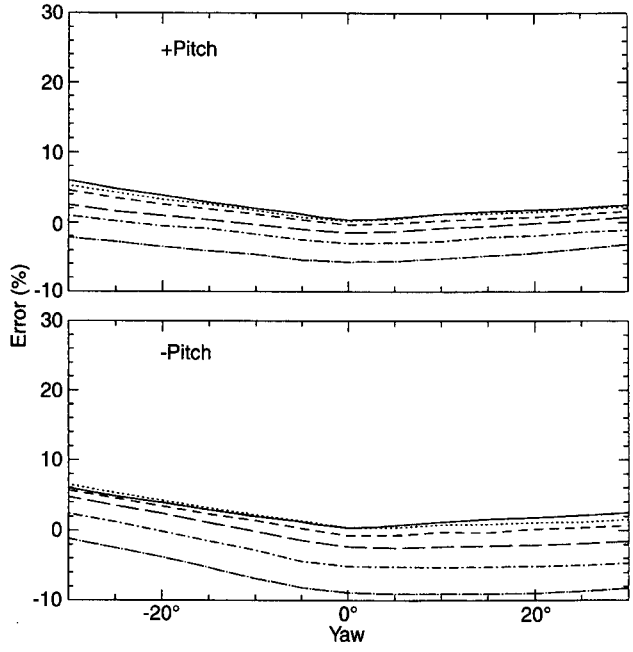

Fig. 3. Error in single hot-wire measurements of the velocity vector magnitude as a function of yaw angle at selected pitch angles (descriptions of symbols are given in Fig. 2)

3.2
X-array hot-wire probe results

This evaluation of the effects of bi-normal cooling on X-array probes was performed by first calibrating the X-array sensor in the manner described above. As in the test with the single-sensor probe, the response of the X-array probe was then determined for a variety of pitch and yaw angles.

Figures 4 and 5 show the errors between the induced velocity components and the velocity components recovered from the X-array probe using the LUT technique. The presence of binormal cooling due to yaw when the sensors are oriented in x–y planes causes an overestimation of the recovered U-velocity component for both positive and negative yaw angles. When the flow direction becomes increasingly binormal, the prongs also assume a less aerodynamic orientation and present a larger cross-sectional blockage area. This increase in

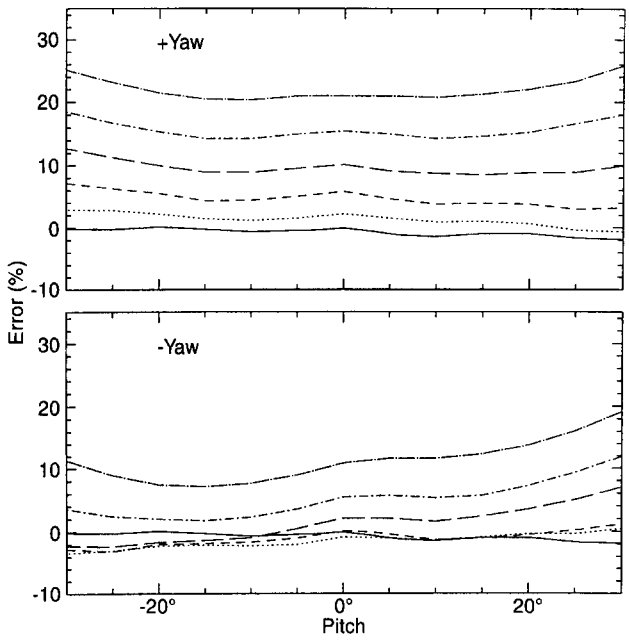

Fig. 4. Error in X-wire measured streamwise velocity component due to binormal cooling at selected yaw angles (descriptions of symbols are given in Fig. 2)

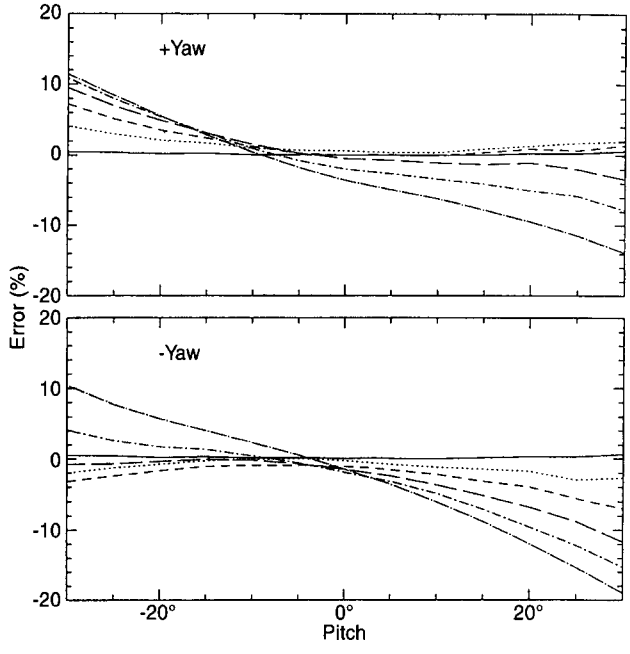

Fig. 5. Error in X-wire measured lateral velocity component due to binormal cooling at various yaw angles (description of symbols are given in Fig. 2)

blockage increases the acceleration of the flow between the prongs, thus cooling the sensors more efficiently. The errors for the present probe were found to be as much as 26% of the induced streamwise velocity component at 25° yaw. The small negative error in the negative pitch and yaw region can be attributed to slight misalignment of the probe in the vertical plane.

As shown in Fig. 5, the magnitude of the measured V-velocity component is also overestimated compared to the induced value when the yaw angle is not zero, i.e. when binormal cooling is present. The relatively smaller percentage error values for the V compared to the U velocity component is somewhat due to the manner in which the percentage errors for V are calculated. Here the measured values are compared to the induced velocity magnitude so that the singularity in calculating the percent error when V is zero is avoided. This should be taken into consideration when reviewing the results. However, the trends in the V results also indicate that larger errors can be expected at high yaw angles when binormal cooling is present. The use of the cosine-law (not shown here) gave less accurate data recovery and did not have a flat error response.

4
Comparison of X-array data reduction techniques

There are basically two methods used to reduce X-wire data. The first, classically known as the cosine-law method, attempts to obtain general empirical description of the cooling of a hot-wire as a function of flow angles. This method had been extensively studied by various researchers and is very well documented in the literature (e.g. Bradshaw 1971; Brunn 1972; Friehe and Schwarz 1968). Using first order approximations and with multiple orientations of the X-probe, previous researchers have been able to approximate the time-averaged, Reynolds shear and normal stresses (e.g. Buresti et al. 1987; Müller 1982). The use of these multi-orientation methods are limited to flows with low turbulence intensities.

The second method, which is the LUT technique and was first introduced by Willmarth and Bogar (1977), simply maps each calibration voltage pair to the two induced velocity components, U and V. Other look-up-table methods include those of Johnson and Eckelmann (1984) and Lueptow et al. (1988). Gresko (1988) further refined the technique of Lueptow et al. (1988) by remapping the calibration map in polar coordinates. Gresko's implementation of the LUT method has been used for the present X-array data reduction and is described briefly below.

In their recent study, Browne et al. (1989) concluded that, for the measurement of instantaneous velocity components in strictly two-dimensional flows, both methods yield similar results in flows with low angles of attack ($\lesssim \pm 15°$) even when the turbulence intensities were high. They found significant deviations from the cosine-law at high angles of attack concurring with the findings of Friehe and Schwarz (1968) and others; and recommended that the LUT method with extended calibration ranges be used for such flows. However, the effects of bi-normal cooling, inherently present in three-dimensional flow fields, was not addressed in their investigation.

4.1
Cosine-law data reduction procedure

The effective cooling velocity (squared) sensed by the probe can be described by a 4th order polynomial fit of the anemometer's output voltage, E:

$$P(E) = U_{\text{eff}}^2 = A_1 + A_2 E + A_3 E^2 + A_4 E^3 + A_5 E^4. \qquad (2)$$

In general, cosine-law methods further decompose U_{eff} into the various components of velocity. In the present implementation, following Jorgensen (1971), for each sensor of the X-array:

$$U_{\text{eff}}^2 = U_n^2 + k_1^2 U_t^2 + k_2^2 U_{bn}^2, \tag{3}$$

where U_n, U_t and U_{bn} are the normal, tangential and binormal velocity components with respect to the sensor coordinate system, as shown in Fig. 1. The coefficients k_1 and k_2 are the pitch and yaw factors, as defined by Jorgensen (1971), which weight the cooling due to the component U_t and U_{bn}. One can also relate these velocity components to the components in the flowfield's coordinate system so that

$$U_n = U\cos\alpha + V\sin\alpha$$

$$U_t = U\sin\alpha + V\cos\alpha,$$

and

$$U_{bn} = W, \tag{4}$$

where α is the angle, shown in Fig. 1, made by the sensor with the x-axis of the flow. More generally,

$$U_n = n_1 U + n_2 V + n_3 W$$

$$U_t = t_1 U + t_2 V + t_3 W$$

and

$$U_{bn} = b_1 U + b_1 V + b_1 W, \tag{5}$$

where n_i, t_i and b_i are the flowfield-sensor coordinate transformation coefficients. However, accurate measurements of the required angles for miniature probes are difficult. Additionally, due to physical effects such as bowed wires and flow blockage due to the prongs, effective angles (see Bradshaw 1971) are not equal to the physical angles. As these effective angles can only be obtained from calibration, it is more convenient to directly calibrate for the combined geometrical-physical coefficients via a modified cooling law from the above equations (e.g. Marasli et al. 1993):

$$U_{\text{eff}}^2 = U^2 + C_1 V^2 + C_2 W2 + C_3 UV + C_4 UW + C_5 VW \tag{6}$$

obtained by substituting Eqs. (5) into Eq. (3) and giving new symbols C_i ($i=1-5$) to the coefficients.

For X-array probes, the terms involving one of the cross-stream components must be eliminated from the above equation so that a determinate coupled set of equations can be formed. In this study, for measurement of the U and V velocity components, the probe is oriented with the wires in the $x-y$ plane. Therefore terms involving W were removed. When combined with Eq. (2) the response equation for each sensor (j) is

$$P(E)_j = U^2 + C_{1j} V^2 + C_{3j} UV, \quad (j=1-2) \tag{7}$$

which can then be solved simultaneously. The coefficients, C_{1j} and C_{2j}, are obtained by a least squares fit of the probe's calibration data.

4.2
Look-up-table data reduction procedure

As for all calibrations involving the use of X-arrays, the LUT calibration procedure involves recording the voltage outputs of the hot-wire anemometers in response to various speeds and flow angles. The LUT method, which is basically an interpolation procedure, requires a much finer calibration grid (i.e. more calibration data points) than the cosine-law method in order to have sufficient resolution. However, as the following results show, the operating angle of attack range is much more extended than that of the cosine-law method.

Gresko's (1988) LUT implementation, used in the present study, remaps the voltage pair for each calibration pitch angle, θ, and speed, Q, into polar coordinates. Figure 6 shows the fan-like plot of the hot-wire voltages (E_1 and E_2) of a typical calibration set. Here, the rationale behind the polar remapping is easily seen. Points along each "arc" represent different pitch angles for a calibration subset at one speed. Calibration subsets with the higher speeds lie on "arcs" with the larger radii. The first step in this procedure is to establish the angular extent of the polar coordinate grid. The lower angular extent is a straight line, $S_{\min}$, that connects the minimum speed and minimum angle voltage pair (Q_1, θ_1) to another minimum angle calibration point (for another speed) such that all other calibration pairs lie above this line. Similarly, the upper angular extent is a second straight line, $S_{\max}$, drawn from the minimum speed and maximum angle voltage pair (Q_1, θ_n) to another maximum angle point such that all other calibration pairs lie below this line. The intersections of lines $S_{\min}$ and $S_{\max}$ is the origin of the polar coordinate system. The hot-wire voltage pairs from the calibration data in the E_1-E_2 cartesian coordinate system are converted to the new polar coordinate system via

$$r = \sqrt{(E_1 - E_{1_{\text{origin}}})^2 + (E_2 - E_{2_{\text{origin}}})^2} \tag{8}$$

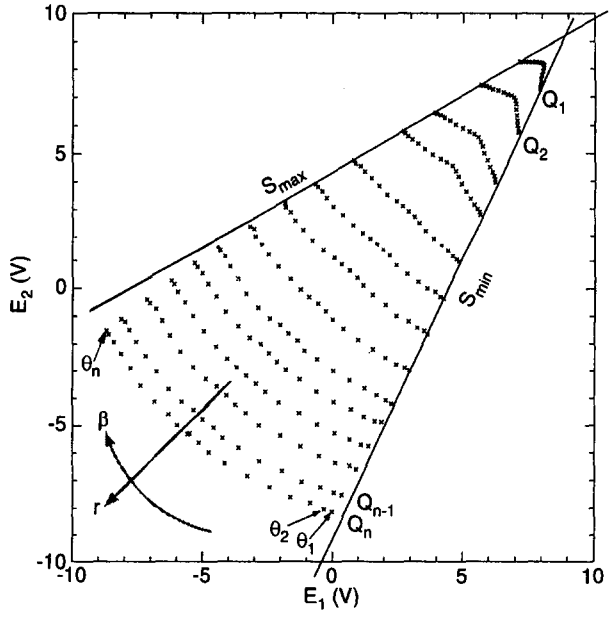

Fig. 6. Typical calibration voltage pairs

and

$$\beta = \tan^{-1}\left[\frac{E_2 - E_{2_{\text{origin}}}}{E_1 - E_{1_{\text{origin}}}}\right], \tag{9}$$

where $E_{1_{\text{origin}}}$ and $E_{2_{\text{origin}}}$ are the voltage values at the intersection of $S_{\min}$ and $S_{\max}$. Then, at constant pitch angle, θ, cubic splines are evaluated so that β and Q are obtained as functions of r. With these cubic splines and at regular intervals of r, β and Q are determined at each θ. Then for each r value, cubic splines are fitted for Q and θ as functions of β. Finally at regular intervals of β, Q and θ are determined, which results in Q and θ values for each r and β, thereby completing the look-up table grid. The values of Q and θ for data points occurring between grid nodes are determined by interpolation.

4.3
Comparison of the Cosine-law vs. LUT technique

Comparisons of the data recovery accuracy between the cosine-law method and the LUT reduction method are plotted in Figs. 7 and 8, for the U and V velocity components, respectively. The plots, for several calibration velocities ranging from 0.5 to 6 m/s, show the difference between the recovered and the induced velocity as a percentage accuracy error that is based on the induced calibration velocity magnitude, V_c. The LUT method shows much better accuracy in data recovery for both velocity components (note the change in % error vertical scale on the plots). The cosine-law method did not converge for calibration velocities below 1 m/s. For this comparison, the calibration coefficients for the cosine-law were obtained from all the available data (i.e. a global fit). At the expense of additional programming complexities, the performance for the cosine-law would probably improve if regional calibration coefficients sets (each for limited calibration speeds and pitch angle ranges) had been used instead. However, with multiple sets of calibration coefficients, transitions at the borders of each calibration range must be carefully handled to avoid data discontinuities.

These comparison plots also show that, especially for the V-velocity component, the errors increase with increasing pitch angle. For calibration velocities of 1 m/s and higher, however, the small LUT error ($\pm 1\%$) is fairly flat across the range of pitch angles shown here. This result concurs with that of Brown et al. (1989), who had also reported that the cosine-law is not accurate for angles above 15° compared to the LUT method. However, the cosine-law data from the present probe converges fairly accurately for flow velocities greater than 2 m/s. This better performance could be due to geometrical and physical differences between the probes used here and that of Browne et al. (1989).

5
4-sensor data reduction technique

A schematic of the 4-sensor hot-wire probe is shown in Fig. 9. Following the discussion in Sect. 4.1 above, the response equations for each of the 4-hot-wires can be written as

$$P_j(E) = U^2 + C_{1j}V^2 + C_{2j}W^2 + C_{3j}UV + C_{4j}UW + C_{5j}VW \quad (j = 1-4). \tag{10}$$

The present data reduction scheme treats the probe as a pair of V-shaped probes, i.e. a vertical pair (consisting of wires 1 and 3) and horizontal pair (consisting of wires 2 and 4). The iterative Newton's scheme, begins by solving for the U and

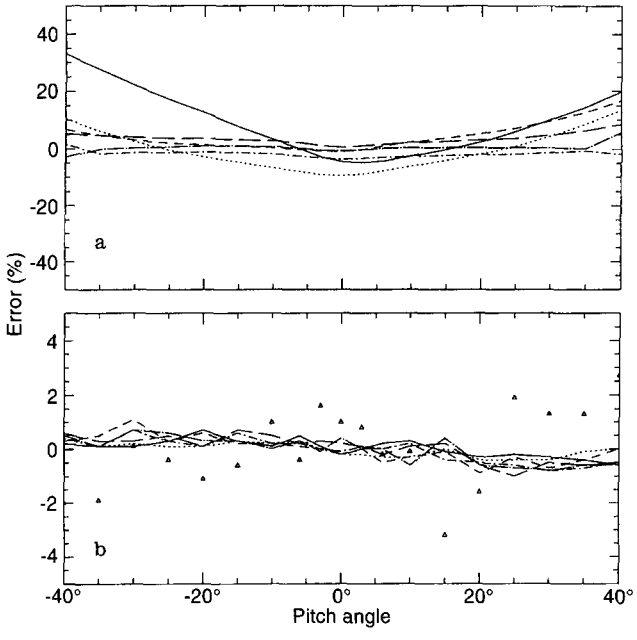

Fig. 7a, b. Error in recovering the induced streamwise velocity component, U, from **a** Cosine-Law method; **b** LUT method, at selected calibration flow speeds, V_c [m/s]: △ 0.5, —— 1, ····· 2, - - - - 3, – – – 4, —·—· 5, — · — 6. (Note the different % Error vertical scales for **a** compared to **b**).

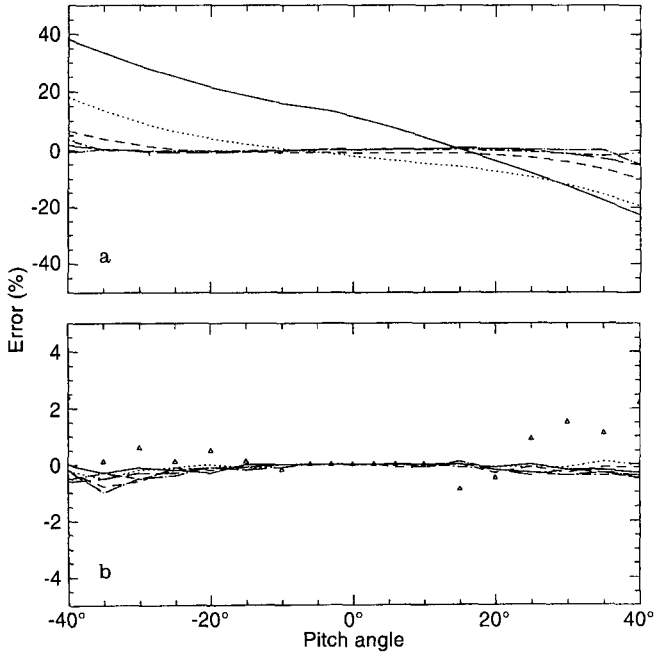

Fig. 8a, b. Error in recovering the induced lateral velocity component, V, from **a** Cosine-Law method; **b** LUT method, at selected calibration flow speeds, V_c [m/s]. (Symbols are described in Fig. 7)

V velocity components using the response equations from the vertical wire pair and with W initially set to zero. The resultant U and V velocity components calculated from the first step are then used in the response equations for the horizontal wire pair to obtain U and W. With each iterative step the latest values for U, and V or W, are used and the process is repeated until the velocity components converge.

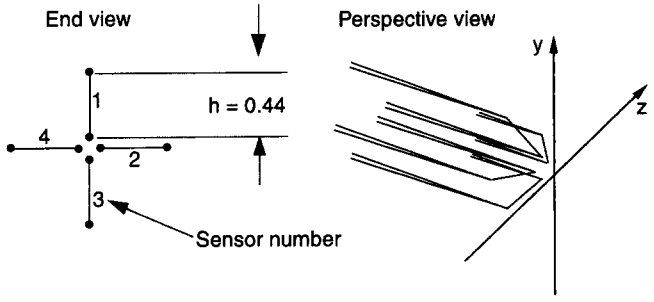

Fig. 9. Schematic of the 4-sensor hot-wire probe (dimensions in mm)

6
Circular cylinder wake measurements

The measured vortex shedding frequency is approximately 64 Hz corresponding to a Strouhal Number, $St \approx 0.21$. With a sampling duration of nearly 120 s at 6912 Hz, each measurement recorded the velocity signatures of approximately 7680 vortex cycles. Although, only half (or 60 s) of the data were necessary to achieve statistical results from each measurement, all 120 s of each data set were used to ensure full converge.

6.1
Mean statistics

The mean $\bar{U}$ and $\bar{V}$, and the rms, skewness and flatness profiles of the u and v fluctuating velocity components, at the various x/d locations, are plotted in Figs. 10 and 11, respectively. The Reynolds shear stress, $\overline{uv}$, profiles are plotted in Fig. 12. Also compared in these figures, where available, are the LES (with the dynamic subgrid scale model and 5th order accurate upwind-biased scheme for the convective fluxes) results of Beaudan and Moin (1994), and the measurements of Zhou and Antonia (1993).

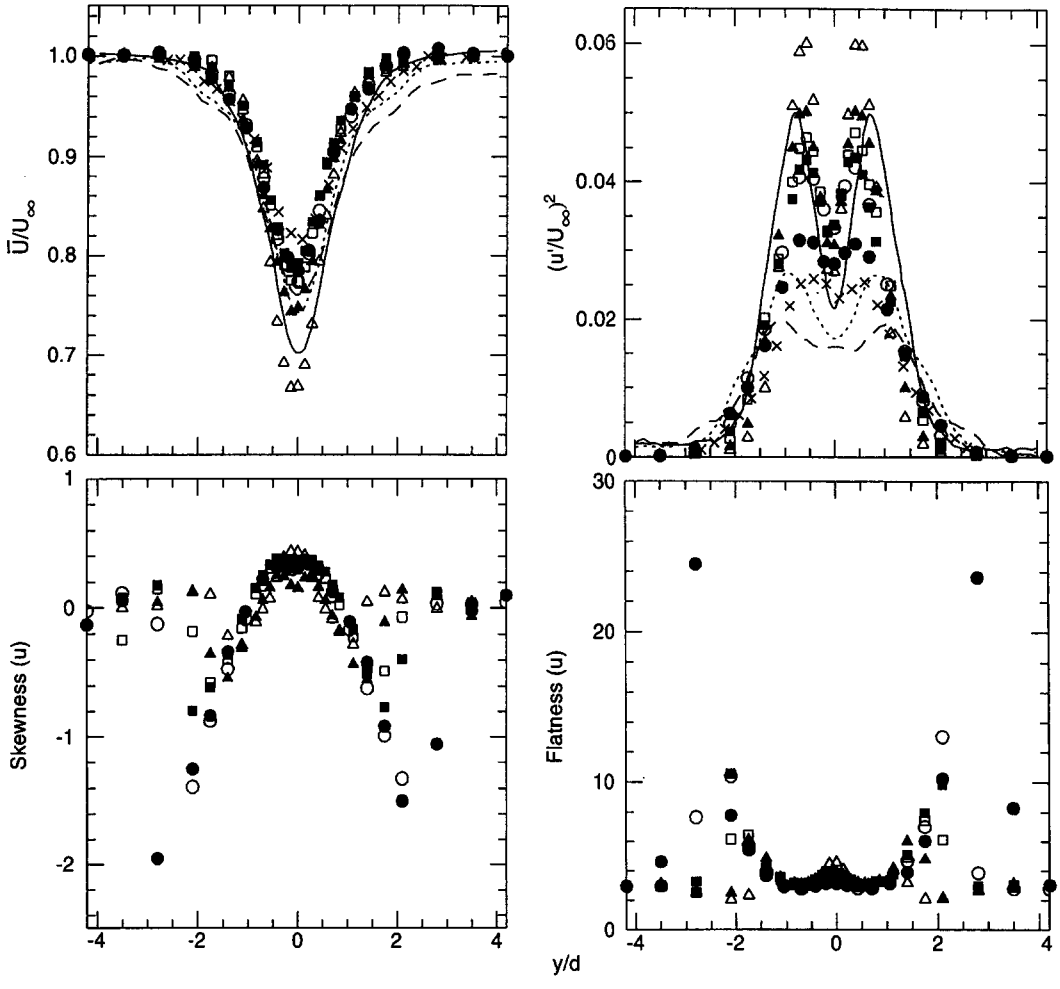

Fig. 10. Mean statistics of the streamwise velocity component at various distances from the cylinder. [Symbol used: x/d] Present data: △ : 3, ▲ : 4, □ : 5, ■ : 6, ◦ : 7, ● : 10: LES (Beaudan et al. 1994): ——4, ····7, - - - 10; Zhou and Antonia (1993): × : 10

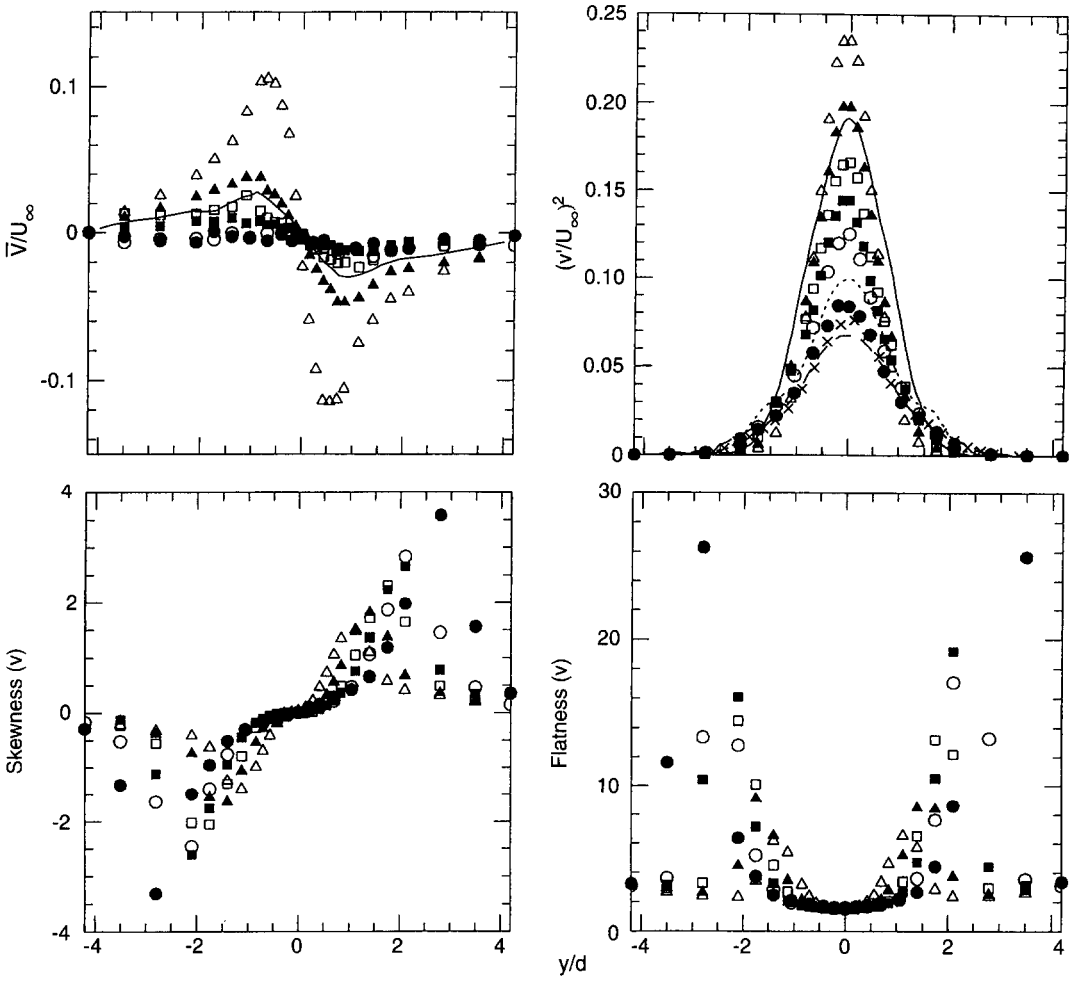

Fig. 11. Mean statistics of the lateral velocity component at various x/d locations (Symbols are described in Fig. 10)

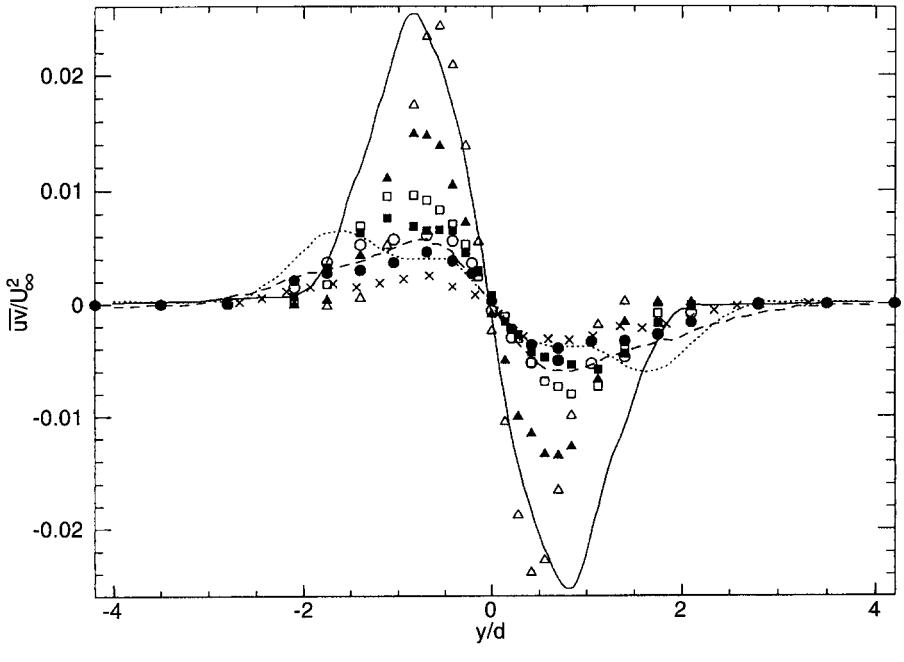

Fig. 12. Reynolds shear stress profiles at various x/d locations (Symbols are described in Fig. 10)

The streamwise velocity component statistics exhibit the expected trend, i.e. with increasing distance from the cylinder: (1) the wake mean velocity deficit decreases, (2) the peaks in the rms of the streamwise velocity component, u', decrease, and (3) the wake spreads, as evidenced by the increased separation of the peaks of the skewness and flatness factors and, to a lesser extent, the rms profiles. These profiles also show excellent symmetry about the wake centerline. As the skewness plots indicate, the largest velocity fluctuations near the center of the wake are positive as evidenced by the positive skewness. Large negative velocity fluctuations occur at the outer edges of the wake as evidenced by the negative skewness. Except at the wake's the outer edges and centerline, the streamwise velocity fluctuations have flatness values quite close to the Gaussian value of 3.0.

In general, it appears that, in comparison to our experimental values, the LES of Beaudan and Moin (1994) overpredicts the centerline velocity deficit. There is relatively good agreement between the LES and the present data in the peak magnitude of the streamwise velocity rms at $x/d=4$. However this velocity statistic is significantly underpredicted by the LES at the downstream locations of $x/d=7$ and 10. By examining the y/d locations of rms peaks in the wake, especially at $x/d=10$, it can be deduced that the LES calculated a slightly wider wake than that of the present experiments as well as that of Zhou and Antonia (1993). Detailed analysis of the discrepancies between the LES and the present data can be found in the comprehensive LES study of Beaudan and Moin (1994). The X-array hot-wire measurements of Zhou and Antonia (1993) at x/d of 10 show a slightly smaller wake deficit than our measurements and somewhat smaller peak rms values.

The lateral velocity component also exhibits the expected trends for a cylinder wake. The antisymmetry of the mean velocity and skewness factor profiles is clearly evident for all x/d locations of the present measurements. Similar to the mean $\bar{U}$ results, the LES yielded lower mean $\bar{V}$ values compared with those of the experiments. As in the case of the u' rms, the v' rms values from the LES at $x/d=4$ compares quite well with the experiments, showing only slight under prediction of the peak magnitude. There are larger differences between the LES v' peak magnitudes and those of the present measurements at the two further downstream locations, $x/d=7$ and 10. The v' measurements of Zhou and Antonia (1993) at x/d of 10 compare quite well to the present measurements except for the peak values near the wake centerline, where their measured peak values lie between those of the present measurements and the LES.

The Reynolds shear stress, $\overline{uv}$, profiles are plotted in Fig. 12. The $\overline{uv}$ peaks decrease in magnitude with increasing distance from the cylinder. These peaks also move further from the centerline due to the widening of the wake at x/d locations

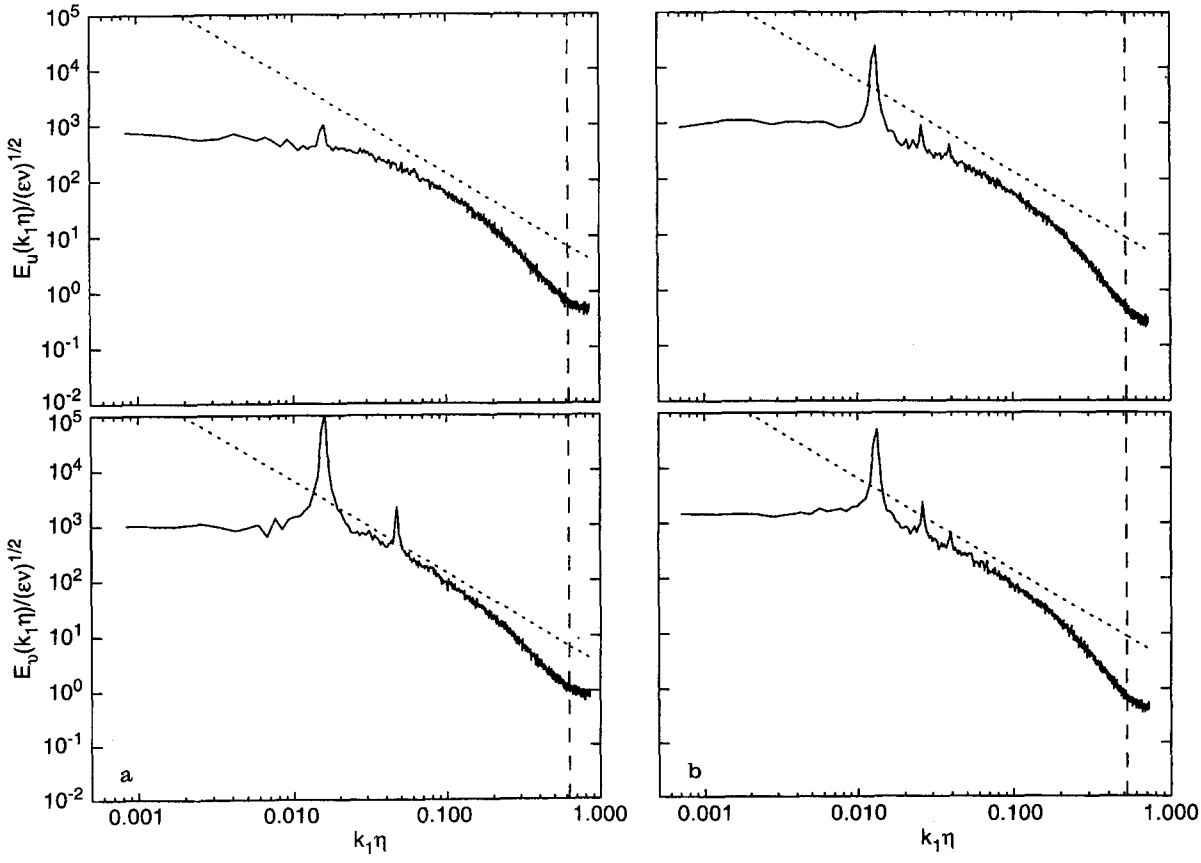

Fig. 13a, b. Spectra of the streamwise and lateral velocity fluctuations at $x/d=3$. **a** $y/d=0$; **b** $y/d=0.56$ (····· −5/3 slope, - - - low-pass filter cut-off frequency)

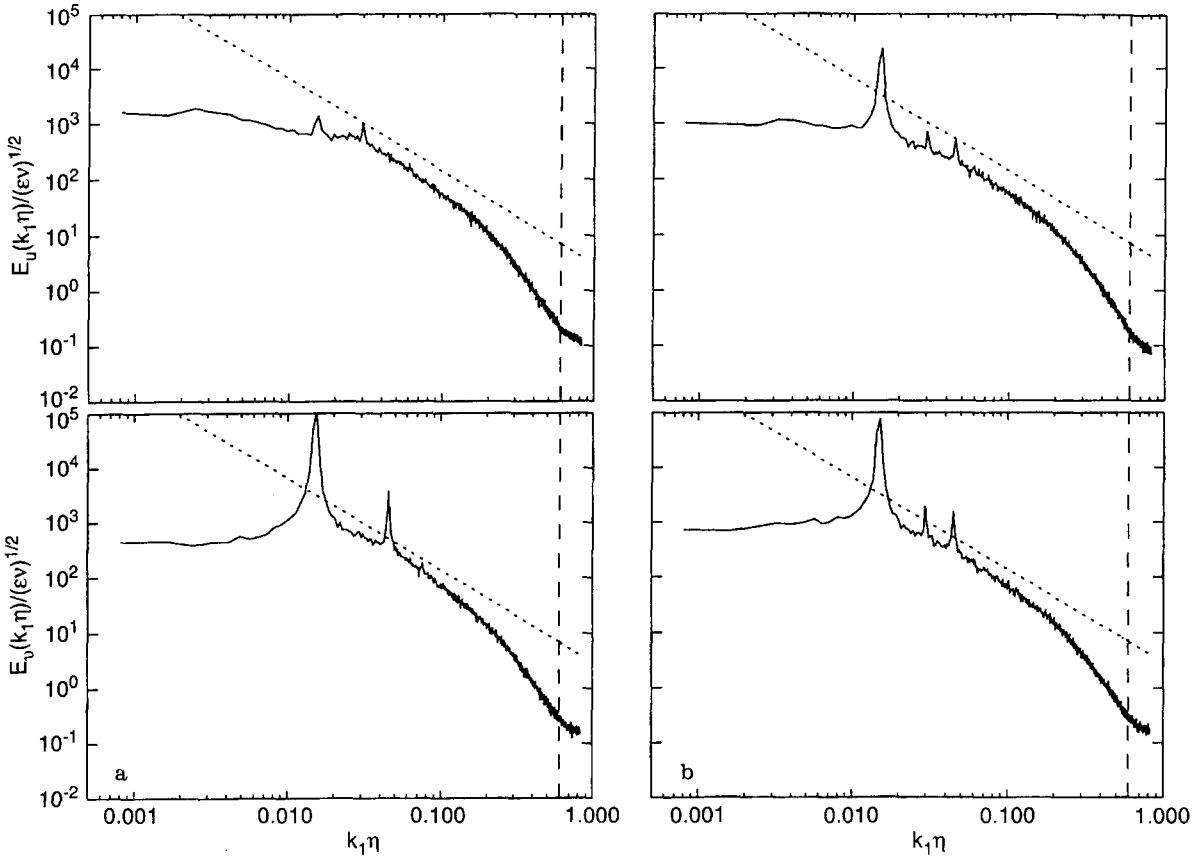

Fig. 14a, b. Spectra of the streamwise and lateral velocity fluctuations at $x/d = 5$. **a** $y/d = 0$; **b** $y/d = 0.42$ (····· −5/3 slope, - - - low-pass filter cut-off frequency)

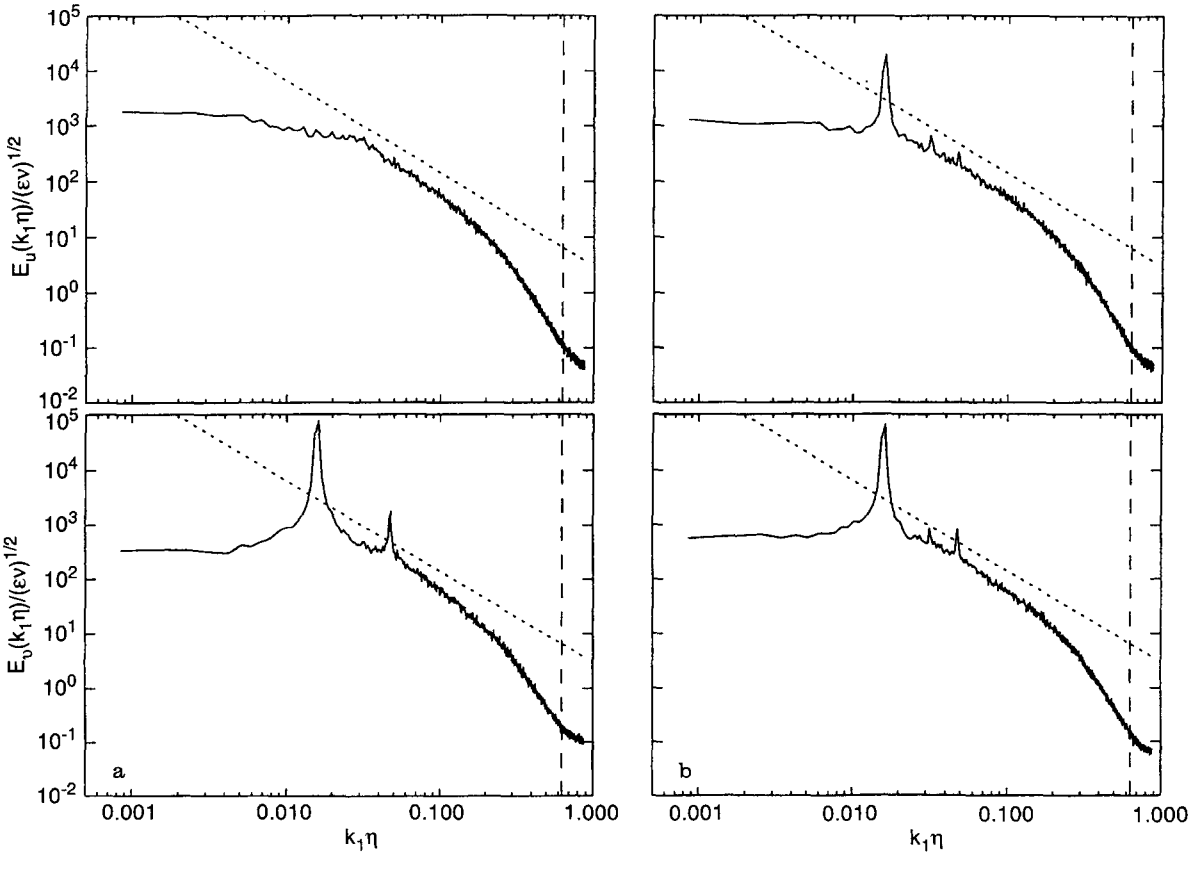

Fig. 15a, b. Spectra of the streamwise and lateral velocity fluctuations at $x/d = 7$. **a** $y/d = 0$; **b** $y/d = 0.42$ (····· −5/3, slope, - - - low-pass filter cut-off frequency)

further from to the cylinder. The LES $\overline{uv}$ profiles agree quite well with the experiments at $x/d=10$. While the LES provided good agreement with the peak magnitudes at $x/d=7$, the $\overline{uv}$ peaks of the LES are further from the centerline, occurring at $y/d \approx 1.75$, compared to our measured peak location of $y/d \approx 0.75$. The least favorable comparison between the LES and the present experiments occurs at the upstream location of $x/d=4$, where the LES overpredicts the $\overline{uv}$ magnitude by about 60%. This contrasts with the mean and rms profiles for the streamwise and lateral velocity components, which show better agreement at this upstream location. The $\overline{uv}$ measurements of Zhou and Antonia (1993) show somewhat smaller peak values than ours, consistent with their smaller peak u' values.

During the course of the present study, it was noted that, when the cosine-law method was initially used to reduce the X-array data (thereby limiting the operational angle of attack to about 20°), the $\bar{U}$ and u' values thereby obtained compared quite well to those of Zhou and Antonia (1993). This implies that velocity vectors of the present wake flowfield which exceed 20° contribute quite significantly to the measured statistical properties.

6.2 Velocity spectra

The one-dimensional k_1 wave number spectra of the u and v velocity components at $x/d=3$, 5, 7 and 10, plotted with Kolmogorov scaling, are shown in Figs. 13–16. These are really frequency spectra that have been converted to wave number spectra with the use of Taylor's hypothesis, with the local mean velocity as the convection velocity. The Kolmogorov length scale, η, used in the normalization was obtained from the isotropic estimate. The $-5/3$ slope on these plots is represented by the dotted line, and the vertical dashed line indicates the location of the low-pass filter cut-off frequency. At each x/d location, the spectra are plotted for the centerline and for the approximate half-wake positions.

At the half-wake locations, the shedding frequency, $f_s=$ 64 Hz, appears as the largest peaks on the spectra for both the u and v velocity components. The u-spectral peaks at each streamwise station becomes very small at the centerline. At $x/d=7$ and 10 these centerline ($y/d=0$) u-spectra peaks are indistinguishable from the background levels. While the first and second harmonics of the shedding frequency also appear clearly in both the u and v spectra at the half-wake locations, the centerline plots of the v-spectra show only the presence of the second harmonic (which appears in the centerline u-spectrum at x/d of 5). These results are consistent with those of Nguyen (1993), who also observed that the occurrances of these fundamental and harmonic peaks can be predicted from linear stability theory.

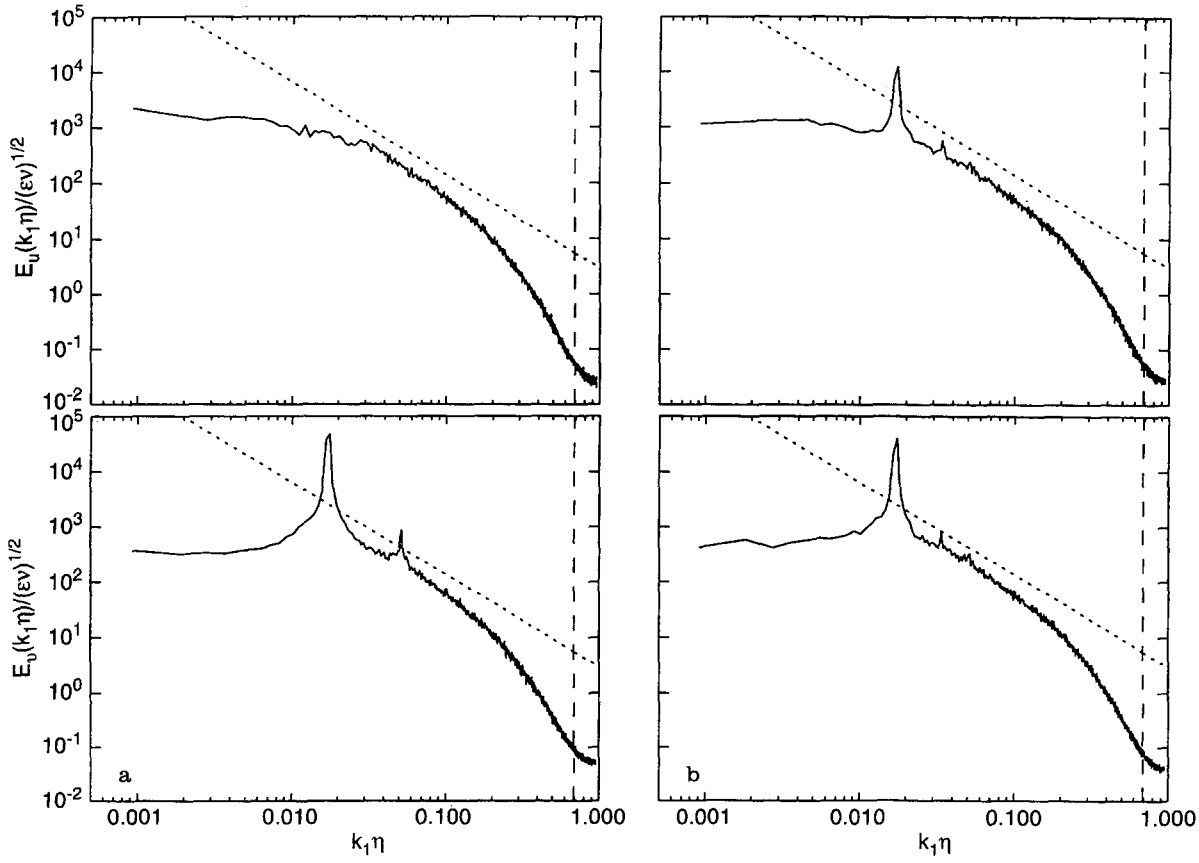

Fig. 16a, b. Spectra of the streamwise and lateral velocity fluctuations at $x/d=10$. **a** $y/d=0$; **b** $y/d=0.7$ (····· $-5/3$ slope, - - - low-pass filter cut-off frequency)

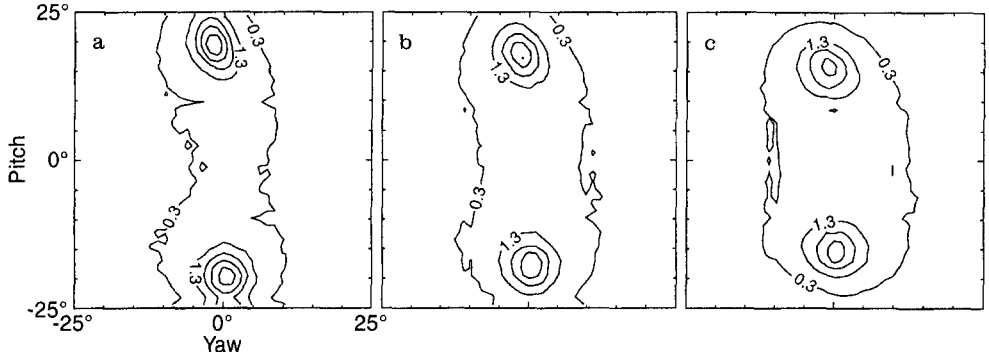

Fig. 17a–c. JPDFs of the pitch and yaw angles along the wake centerline **a** $x/d=5$; **b** $x/d=7$; **c** $x/d=10$. (The contour levels values have been multiplied by a factor of 10^3)

7
4-sensor hot-wire probe measurements

The X-array measurements results shown above assume and require that the flow is dominantly two-dimensional, because they necessarily neglect binormal cooling. This set of 4-sensor probe measurements was made to explore the extent of three-dimensionality of the very near wake region and thus, semi-quantitatively, to verify the accuracy of the X-array measurements. These measurements were made at locations along the wake centerline where it was expected that three-dimensional effects are most pronounced. Limited by the operational range of the 4-sensor probe of less than 25°, the closest measurement position achieved without significant data loss was x/d of 5.

Figure 17 shows the joint-probability distribution functions (JPDFs) of the measured pitch and yaw angles at $x/d=5$, 7 and 10. At $x/d=10$, the peaks of the contours are at approximately $\pm 15°$ pitch. At $x/d=5$, the position of the peaks in the contours increase to approximately $\pm 20°$ pitch. This trend is consistent with the increase in velocity vector angle of attack as distance from the cylinder decreases, and also illustrates the necessity for the extensive large angle calibration procedure undertaken here for the X-wire measurements. While this plot shows that the data contains large pitch angles of greater than 20°, the contours appear to be contained within yaw angles of approximately $\pm 12.5°$, with most of the data occuring within yaw angles of $\pm 5°$. This demonstrates that the flow is fairly two-dimensional at these locations, thus verifying that the X-array can be used for reasonably accurate measurements in this flowfield.

8
Conclusion

This study has confirmed that single sensor hot-wire probe measurements of the streamwise velocity component are not accurate for flowfields with large non-zero cross-stream components. Similarly, X-array measurements of the U and V velocity components in flows containing large W are also subject to large errors resulting from unaccounted for binormal cooling.

Using the LUT technique, and by calibrating the X-array probe used here to include the range of pitch angles ($\pm 40°$) expected in the flow, accurate X-array measurements of instantaneous U and V velocity components in the very near wake region of a circular cylinder (x/d of 3 to 10) at $Re_d \approx 3900$ have been accomplished. The approximate two-dimensionality of the present flowfield was verified with 4-sensor probe measurements. Hence, binormal cooling errors in the present X-array measurements are small.

References

Achenbach E (1968) Distribution of local pressure and skin friction around a circular cylinder in cross-flow up to $Re=5\times10^6$. J Fluid Mech 34: 625–639

Beaudan P; Moin P (1994) Numerical experiments on the flow past a circular cylinder at subcritical Reynolds number. Technical Report TF-62, Stanford University, Thermal Sciences Div., Dept. of Mechanical Engineering

Bloor M; Garrard J (1966) Measurements on turbulent vortices in a cylinder wake. Proc Royal Society A 294: 319–342

Bouard R; Coutanceau M (1980) The early stage of development of the wake behind an impulsively started cylinder for $40<Re<10^4$. J Fluid Mech 101: 583–607

Bradshaw P (1971) An Introduction to Turbulence and its Measurement. Pergamon, NY

Browne L; Antonia R; Chua I (1989) Calibration of X-probes for turbulent flow measurements. Exp Fluids 7: 201–208

Brunn H (1972) Hot-wire data corrections in low and high turbulence intensity flows. J Phys E: Sci Instrum 5: 812

Buresti G; Di Cocco NR (1987) Hot-wire measurement procedures and their appraisal through a simulation technique. J Phys E: Sci Instrum 20: 87–99

Cantwell B; Coles D (1983) An experimental study of entrainment and transport in the turbulent near wake of a circular cylinder. J Fluid Mech 136: 321–374

Champagne F; Sleicher C; Wehrmann O (1967) Turbulence measurements with inclined hot-wires. Part 1. Heat transfer experiments with inclined hot-wire. J Fluid Mech 28: 153–176

Champagne F; Sleicher C (1967) Turbulence measurements with inclined hot-wires. Part 2. Hot-wire response equations. J Fluid Mech 28: 177–182

Farell C; Blessmann J (1983) On critical flow around smooth circular cylinders. J Fluid Mech 136: 375–391

Friehe C; Schwarz W (1968) Deviations from the cosine law for yawed cylindrical anemometer sensors. J Appl Mech 655–662

Gresko Jr LS (1988) Characteristics of wall pressure and near-wall velocity in a flat plate turbulent boundary layer. Master's thesis, Massachusetts Institute of Technology

Johnson FD; Ecklemann H (1984) A variable angle method of calibration for X-probes applied to wall bounded turbulent shear flow. Exp Fluids 2: 121–130

Jorgensen F (1971) Directional sensitivity of wire and fiber-film probes. In: DISA information. Vol. 11, p. 31. DISA Electronics

Leuptow LM; Breuer KS; Haritonidis JH (1988) Computer aided calibration of X-probes using a look-up table. Exp Fluids 6: 115–118
Marasli B; Nguyen P; Wallace J (1993) A calibration technique for multiple-sensor hot-wire probes and its application to vorticity measurements in the wake of a circular cylinder. Exp Fluids 15: 209
Müller UR (1982) On the accuracy of turbulence measurements with inclined hot wires. J Fluid Mech 119: 155–172
Nguyen PN (1993) Simultaneous measurements of the velocity and vorticiity fields in the turbulent near wake of a circular cylinder. Ph.D. Dissertation, University of Maryland
Roshko A (19954) On the development of turbulent wakes from vortex streets. Technical Report 1191, National Advisroty Committee for Aeronautics (NACA)
Townsend A (1947) Measurements in the turbulent wake of a cylinder. Proc Roy Soc 190 A: 551–561
Townsend A (1949a) The fully developed turbulent wake of a circular cylinder. Australian J Sci Res 2A: 451–468
Townsend A (1949b) Momentum and energy diffusion in the turbulent wake of a cylinder. Proc. Roy Soc 197: 123–140
Willmarth W; Bogar T (1977) Survey and new measurements of turbulent structure near the wall. Phys Fluids 20: S9–S21
Wygnanski I; Champagne F; Marasli B (1986) On the large scale structures in two-dimensional, small deficit wakes. J Fluid Mech 168: 31–71
Yamada H; Kuwata Y; Osama Y (1989) Turbulence measurements in a two-dimensional turbulent wake. Technical Report 4, Yamaguchi University, Japan.
Zhou Y; Antonia R (1993) A study of turbulent vortices in the near wake of a cylinder. J Fluid Mech 253: 643–661

Announcements

7th International Conference

Laser Anemometry Advances and Applications

University of Karlsruhe, Germany September 8–12, 1997

Objectives and scope
The conference is the 7th in a series on the topic of Laser Anemometry. Preceding conferences were held in the UK at the Universities of Manchester, Strathclyde, Swansea, in the USA in Cleveland and in Hilton Head Island, and in NL in Veldhoven. The 7th Conference will again provide an excellent opportunity for engineers and scientists to present and discuss new developments in the field.

Topics
- Development of all forms of point and whole field measuring laser anemometers (LDA, L2F, PDA, P2F, PTA, PIV, DGV, LIF ···).
- Application of these techniques to single phase and multiphase flows, unsteady and separated flows, high speed flows, biomedical flows, combustion and reacting flows, atmospheric boundary layer flows, rotating and reciprocating machinery, particle sizing.
- Comparison of laser-based experimental results with numerical codes

Note that this list is not meant to be exhaustive and that papers in other subject areas will be considered.

Paper submission
Authors should submit three (3) copies of an extended abstract of not less than 700 words, with supporting figures as appropriate, to the conference chairman (B. Ruck). The covering letter should contain: 1) title of the paper, 2) name, address, phone and fax number, 3) keywords to describe and categorize the work easily. The acceptance of the papers will be based upon reviews of the extended abstracts. The papers will be published in a bound Proceedings Volume. Final acceptance for publication in the Proceedings Volume will depend on complete camera-ready paper preparation. The Proceedings Volume will be available at the time of the conference. The official language of the conference will be English. In all cases, work must be original and should not have been published nor offered for publication elsewhere.

Exhibition
An exhibition is planned to enable participating companies to bring their products to the attention of potential customers. Further details are available on request.

Location
The conference will be held on the campus of Karlsruhe University, Germany. Karlsruhe University is the oldest technical university in Germany. Karlsruhe is located in the river Rhine valley in the immediate vicinity of the Black Forest. The city is the economic and scientific metropolis of the central Upper Rhine region. September is a season with usually pleasant temperatures and predominantly (not exclusively) nice weather conditions.

Deadlines
November 15, 1996: 3 copies of extended abstract due January 15, 1997: Notification of paper acceptance May 15, 1997: Full-length paper due

Enquiries and all correspondence should be addressed to:
Dr. B. Ruck
Institut für Hydromechanik
Universität Karlsruhe
Kaiserstraße 12 D-76128 Karlsruhe Germany
Telephone & Fax: +49 721 608 3897